REFLECTS – A EUROPEAN CRAFT PROJECT FOR THE DEVELOPMENT OF A BIFACIAL SILICON SOLAR CELL MODULE

B. Terheiden[1], P. P. Altermatt[1,2], R. Meyer[1], R. Brendel[1], J. Janusonis[3], L. Leonas[3], S. Tselepis[4], B. Clive[5], E. Zilinskas[6], W. Koornstra[7], S. Evans[8], H. van Ekelenburg[9], A. Elazari[10], A. Badham[11]
[1]*Institut für Solarenergieforschung Hameln/Emmerthal (ISFH), Am Ohrberg 1, 31860 Emmerthal, Germany,*
[2]*University of Hannover, Dep. Solar Energy Research, Appelstr. 2, 30167 Hannover, Germany*
[3]*Institute of Lithuanian Scientific Society, A. Costauto str. 11-466, 01108 Vilnius, Lithuania*
[4]*Centre for renewable energy sources,19th km Marathonos Ave, 19009 Pikermi, Greece*
[5]*Optical Products ltd., 74-75 Brunner Road, London E17 7NW, Great Britain*
[6]*Saules Energija, LT-49362 Kaunas, Lithuania,*
[7] *GiraSolar, Munsterstraat 9, 7418EV-Deventer, The Netherlands*
[8]*Heavens Solar Technology, 74 Main Street,Mexborough, South Yorkshire, S64 9EA, Great Britain*
[9]*Pro Support,P.O. Box 563, 7550 Hengelo, The Netherlands*
[10]*Millennium Electric Ltd., P.O. Box 2646, Raanana, Israel 43650*
[11] *Badham Farms, Woodland Hall Farm, Wood Lane, Uttoxeter, Staffs, ST14 8JS, Great Britain*

ABSTRACT: The objective of the REFLECTS project (Novel bifacial single substrate solar cells utilising reflected solar radiation) is the development of a cost effective, high efficiency bifacial silicon solar module exploiting the light reflected from behind the cells for energy generation. A bifacial rear contact silicon solar cell using a simple processing sequence is developed. Mechanical grinding is deployed for the definition of the emitter and base contact regions. The rear surface structure is then utilised as a mask for the self-aligned metallization of the bifacial rear contact cells applying the OECO (obliquely evaporated contacts) – technique. We achieved an efficiency of 20.5 % under illumination from the non-metallised cell side whereas the efficiency is as high as 17.0 % when illuminated from the metallised side. A string of 5 bifacial cells is mounted and encapsulated on a non-concentrating reflector developed within the project. Applying the reflector enhances the short circuit current by 38 %.
Keywords: bifacial, back contact, optical simulation

1 INTRODUCTION

Bifacial solar cells are sensitive to illumination on the front as well as on the rear side. In front of a highly reflective background e. g. white walls bifacial solar cells can produce up to 50 % more energy per cell area compared to monofacial solar cells [1, 2]. The alignment of those cells relative to the sun is for a large range of azimuth angles possible without significant energy losses. Thus an installation in north-south direction gives about the same energy output as one with east-west orientation. Additionally the daily energy production is homogeneous without a predominant maximum at noon.

The first bifacial solar cell was introduced 1960 [3]. Hübner et al. developed a bifacial silicon solar cell (4 cm^2) with an efficiency of 20.1 % under front and 17.2 % under rear side illumination [4]. The above mentioned bifacial solar cells feature a front junction and thus a front and rear contact grid. Rear contact silicon solar cells are of bifacial design. Glunz et al. demonstrated 1997 a rear contacted bifacial solar cell with 20.6 % and 20.1 % front and rear side efficiency respectively [5]. Applying a highly sophisticated solar cell process Othsuka et al. presented a bifacial solar cell of an efficiency of 21.3 % and 19.8 % for front and rear side, respectively on an area of 1 cm^2 [6]. A different approach is the Sliver® solar cell concept. This very thin (thickness < 100 µm) bifacial silicon solar cells show an efficiency of above 19 % from both sides [7]. Müller et al. presented a bifacial, rear contacted solar cell called the Back OECO (obliquely evaporated contacts) Si solar cell in 2005. An independently confirmed efficiency of 21.5 % under front side illumination and 17.7 % under rear illumination has been achieved [8].

The approach of the REFLECTS project is the parallel development of a rear junction, rear contact bifacial solar cell and a suitable reflector. The aim is to develop a highly efficient bifacial solar cell based on a simple processing sequence incorporating structuring by mechanical abrasion using a conventional dicing saw and reflector feasible for mass production.

2 CELL DESIGN

Figure 1 shows a photograph of the bifacial rear contact silicon solar cell produced within the REFLECTS project.

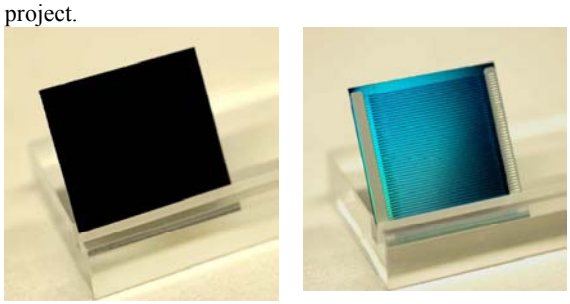

a) b)

Figure 1**:** Photograph of the bifacial rear contact solar cell produced in the REFLECTS project. The difference in the thickness of the antireflective coating is smaller in reality.

The non-metallized “front” side (Figure 1a) is textured showing randomly arranged upright pyramids, no shading due to metal contacts arises. On the metallized “rear” side (Figure 1b) the contact fingers of emitter and base are interdigitatedly placed. Highly phosphorous and boron doped regions are introduced

beneath the metal contacts respectively. The predominant feature of this bifacial solar cell is the definition of the highly doped regions by means of mechanical abrasion using a conventional dicing saw.

The metallization is carried out applying the so called obliquely evaporated contacts [9]. This technique uses the structured Si wafer surface as a mask allowing for self aligned contact finger evaporation on the vertical flanks of the mechanically grinded grooves. The bottom of the grooves is not metallised. The contact area is determined by the angle under which the metal reaches the wafer surface as well as the width of the grooves.

The busbars running perpendicular to the fingers are evaporated through a shadow mask.

When illuminated from this metallised cell side the advantage of this technique comes into play. Since the metal fingers are placed on the vertical flanks the shadowing is only given by the finger thickness but not by the finger width as it is the case for conventional metallization techniques. The bifacial cell has a SiN anti reflective coating on both sides.

For maximum yearly performance the bifacial solar cells are mounted on a suitable reflector.

3 TWO-DIMENSIONAL DEVICE SIMULATIONS

In Figure 2 the simulated efficiency of bifacial cells with a structured rear side in dependence of the wall width between adjacent emitter and base grooves is demonstrated. The numerical simulation program DESSIS is applied [10]. The width of base and emitter grooves is the same optimised separately for each bulk lifetime. As parameters different groove depths and bulk lifetimes are considered. The groove depths are chosen 40 µm, 80 µm and 120 µm, whereas the bulk lifetimes are 10 µs, 40 µs, 100 µs and 500 µs.

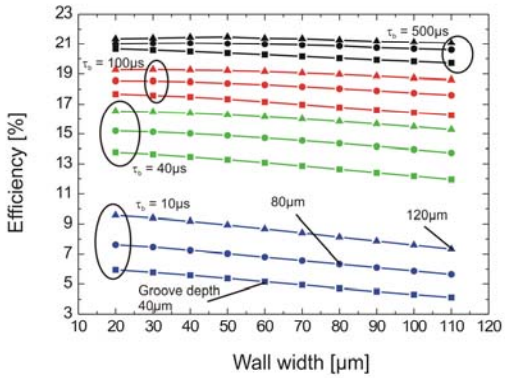

Figure 2: Efficiency vs. width of walls between emitter and base groove. The cell is illuminated from the non-metallised side. The geometry is assumed to be symmetric e. g. the same width of base and emitter grooves.

In this simulation the wafer thickness is 330 µm and the base resistivity is 0.6 Ωcm. The effective surface recombination velocity is 30 cm/s for the base surface and 2000 cm/s for the n^+ and p^+ regions. The emitter depth is chosen as 0.4 µm and the sheet resistance 90 Ω/sq, while the boron back surface field is 0.8 µm deep at a sheet resistance of 100 Ω/sq.

From Figure 2 we deduce that the impact of the wall width on the efficiency is the smaller the higher the bulk lifetime is. The increase in efficiency due to deeper emitter and base grooves is the higher the lower the bulk lifetime is. Both effects are due to the enhanced charge carrier collection probability due to smaller distances between the location of generation and the pn-junction. But there is even for bulk lifetimes of 500 µs an enhancement in efficiency.

4 PROCESSING SEQUENCE

The process development is carried out on (100)-oriented, 3.5 Ωcm *p*-type float-zone Si wafers of a thickness of 300 µm. The aperture area of the cells is 3.92 cm^2. The key process steps are the groove formation itself, the metallization and the module fabrication.
The order of the processing steps is chosen according to our OBNP (Oxide, B-diffusion, SiN deposition, P-diffusion)-sequence [11]. The OBNP-sequence avoids boron depletion during P-diffusion and allows for high bulk lifetimes which are essential for rear junction solar cells.

Starting with a thermal oxidation and a SiN coating as a diffusion barrier the base contact grooves are cut for the subsequent B-diffusion after the saw damage removal. Protecting additionally the boron diffused regions the emitter contact grooves are formed. Following the "front" side texturization the surface is passivated by a SiN layer serving also as an anti reflective coating. The metallization is carried out by evaporating Al under a shallow angle forming the contact fingers. The busbar metals, Al and Ag, are evaporated through a shadow mask placed at the end of the contact fingers of the particular polarity of the interdigitated contact grid.

4.1 Groove formation

Optimising the groove geometry different aspects have to be taken into account. For a high minority charge carrier collection probability the width of the emitter grooves shall be wide while the base grooves are kept as narrow as possible. Both types of grooves but in particular the base grooves are carried out as shallow as possible to keep the rear surface area as small as possible. These requirements in combination with the angle of evaporation determine the contact finger width. Additionally technological constraints are also to be taken into account. Hence a minimum distance of 65 µm between the grooves is necessary to achieve mechanically stable walls separating adjacent grooves.

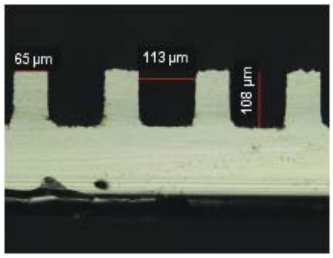

Figure 3: Optimisation of groove formation with regard to obtaining rectangular shaped grooves.

The groove orientation and the crystal orientation are aligned to produce vertical flanks of the grooves after

alkaline saw damage etch. Figure 3 shows the grooves oriented 30° to the flat of the (100) wafer. Here the etching with KOH-solution gives the desired rectangular shape of the grooves. The vertical flanks are necessary for a reliable metallization.

The depth and the width of the grooves in Figure 3 are not the same as for the bifacial cells. For the bifacial cell presented in this work the grooves are 70 µm and 110 µm wide for base and emitter regions respectively. The emitter grooves are 80 µm deep in contrast to the base grooves which are only 40 µm deep. The walls between adjacent grooves are 75 µm thick.

4.2 Metallization

The obliquely evaporation (OECO) technique is based on evaporating metal under a shallow angle onto a structured surface which serves as a mask. Generating structures as for these bifacial cells the plateaus as well as the vertical flanks are metallized but the Al on the plateaus is selectively etched away. The degree of selectivity is dependent on the difference in morphology between Al on plateaus and on the vertical flanks. The morphology is affected by the angle of evaporation.

The angle between metal source and vertical flank of the groove has been optimised aiming at the widest fingers at a given groove width while considering the reliability of the selectivity of the etching process. The largest finger width is given by the groove depth.

5 MODULE FABRICATION

5.1 Interconnection

The bifacial cells are only contacted at the rear side. A string of 5 cells each of the cells has an area of 2.5×2.5 cm^2 is formed using standard soldering techniques.

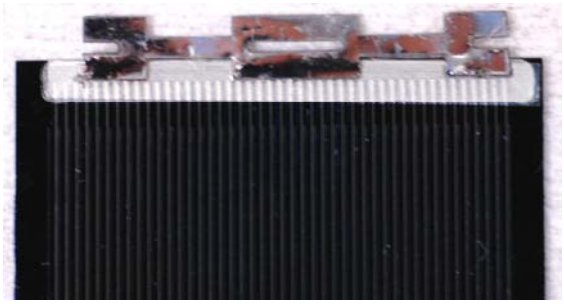

Figure 4: Metallised rear side of the bifacial cell fabricated within the REFLECTS project. The busbar connects the obliquely evaporated contact fingers. The connector bone is soldered to the unstructured part of the evaporated busbar.

The connector bone as displayed in Figure 4 is designed and produced inhouse. The material is tinned copper. The geometry allows balancing the expansion of the different materials in the module.

5.2 Encapsulation

A string of 5 bifacial rear contacted cells is mounted onto a rigid reflector developed within the REFLECTS project. The solid reflector shows a ditch of about 2 mm depth and 2.7 mm width over the entire reflector length where the cell string is placed covered by ethylene vinyl acetate for encapsulation. The cells are encapsulated without a front glass. The rigid reflector gives the mechanical stability.

The shape of the reflector is optimised by means of ray-tracing with the software OptiCAD [12]. For this, we calculate a light source that represents the sun smeared on the blue sky over an entire year as shown in Figure 5. The angular distribution of radiation is projected on the module's front surface while the module is assumed to face south to the celestial equator. The photon flux in dependence of the sun's elevation angle above horizon is calculated with the atmospheric model SMARTS [13]. Thereby, Gueymard's am0 spectrum is used [14] to calculate the standard am1.5g spectrum, as recommended by the ASTM [15]. This spectrum's photon flux is integrated over wavelength from 300 to 1200 nm where Si absorbs. See Figure 6.

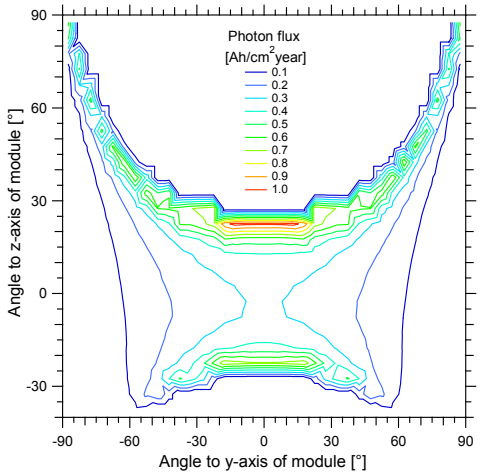

Figure 5: Calculated angular distribution of the sun's photon flux, averaged over the blue sky during an entire year, projected on a module pointing south to the celestial equator. See also Figure 6.

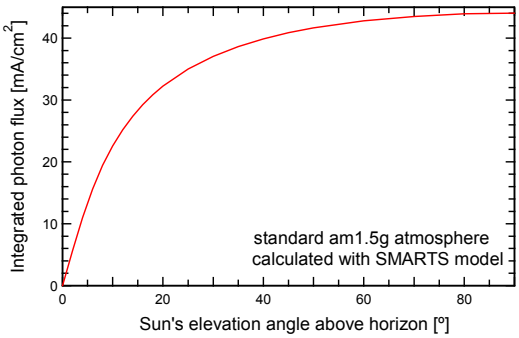

Figure 6: The sun's photon-flux as a function of the sun's elevation angle above horizon, integrated over wavelength from 300 to 1200 nm, where Si absorbs. Calculations of the standard am1.5g spectrum made with SMARTS.

The optical properties of the reflector are measured and served as input for the ray tracing simulation. With the shape obtained from ray tracing the light collection efficiency is close to 80 %. With this geometry about half of all photons are incident on the central part of the

reflector which is a good result considering that the sun is smeared over the entire sky over the entire year.

6 RESULTS

6.1 Cell performance

The highest cell efficiency obtained is 20.5 % (aperture area 3.92 cm^2) when illuminating the non-encapsulated cell from the non-metallised side. The short circuit current density is as high as 41.1 mA/cm^2, the open circuit voltage is 637 mV and a fill factor of 78.3 % is obtained. When illuminating the cell from the metallised side the efficiency is still 17.0 % with an open circuit voltage of 630 mV, a short circuit current density of 34.8 mA/cm^2 and a fill factor of 77.5 %. These cell parameters are among the highest of rear contacted bifacial silicon solar cells processed without applying photolithography. Table 1 summarises these parameters.

Table 1: Cell parameters from illuminated IV-measurements. The bifacial cell is illuminated from the non-metallised and metallised cell side.

Illumination side	V_{OC} [mV]	J_{SC} [mA/cm^2]	FF [%]	η [%]
unmetallised	637	41.1	78.3	20.5
metallised	630	34.8	77.5	17.0

The short circuit density of 41.1 mA/cm^2 shows the advantage of rear contact solar cells. There are various reasons for the lower short circuit current when illuminating the cell from the metallised side: the shading by the OECO-contacts, the absence of a surface texture, the free carrier absorption in the highly doped regions in particular in the highly boron doped regions, recombination at the metal contacts and the surfaces in particular the SiN coated highly boron doped grooves, and a non-optimum antireflective coating. Improvements have to start there.

As deduced from dark and illuminated IV measurements the fill factor should increase when lowering the saturation current of the second diode. The series resistance is below 0.6 Ωcm^2.

6.2 Prototype module performance

The module performance is measured with a CLASS A solar cell tester. The efficiency of the prototype module determined at standard testing conditions is 13.4 %. The reasons that we observe a lower performance of this first module than the individual solar cells show are partly due to the deformation of the reflector during the encapsulation process as well as a non-optimised soldering process for cell interconnection. Both effects compromise the optimised optics of the reflector. Consequently, the optics is not working as optimal as designed. Therefore, comparing the short circuit current of the same string before and after encapsulation the current is enhanced by only about 38 %. The effective surface area of the module, considering the active part of the reflector surface, is increased by a factor of 2.05. Potentially, the reflector is able to increase the short-circuit current after encapsulation by 80 % despite its very shallow and lightweight design.

7 SUMMARY

A process for the fabrication of bifacial rear contact silicon solar cells is developed. The key steps are the mechanical grinding of the grooves to define the emitter area as well as the emitter and base contact regions and the OECO-technique for a self aligned metallization.

The highest cell efficiency obtained is 20.5 % when illuminating the bifacial rear contact cell from the non-metallised side. An efficiency of 17.0 % is achieved when illuminating the cell from the metallised side. These efficiencies are among the highest for bifacial silicon solar cells which are processed without using photolithography.

When mounting a string of 5 of these cells onto a rigid prototype reflector without a front glass the short circuit density is enhanced by about 40 %. The reflector is not concentrating.

Further development of the cell geometry is necessary to overcome the above mentioned drawbacks of the current bifacial cell design.

8 ACKNOWLEDGEMENTS

We thank Mihail Manole for his valuable contribution to this work and Anja Lohse for her reliable solar cell processing. We are also grateful to Maren Gast who built the module. The financial support provided by the European Union within the FP6 under contract no. COOP-CT-2004-513046 is gratefully acknowledged. The ISFH is a member of the German *Forschungsverbund Sonnenenergie*.

9 REFERENCES

[1] R. Hezel, *Novel applications of bifacial solar cells*, Prog. Photovolt. Res. Appl. **11**, 549 (2003)

[2] M. J. Stocks, K. J. Weber, A. W. Blakers, J. Babaei, V. Everett, A. Neuendorf, M. J. Kerr and P. Verlinden, *65-micron thin monocrystalline silicon solar cell technology allowing 12-fold reduction in silicon usage*, Proc. 3rd World Conference Photovoltaic Energy Conversion, xxx (2003)

[3] H. Mori, *Radiation energy transducing device*, U.S. Patent 3.278.811, Oct. 1966, (submitted 1960), (1960)

[4] A. Hübner, A. G. Aberle and R. Hezel, *20 % efficient bifacial silicon solar cells*, Proc. 14th European Photovoltaic Solar Energy Conference, 92 (1997)

[5] S. W. Glunz, J. Knobloch, D. Biro and W. Wettling, *Optimised high-efficiency silicon solar cells with J_{SC} = 42 mA/cm² and η = 23.3 %*, Proc. 14th European Photovoltaic Solar Energy Conference, 392 (1997)

[6] H. Othsuka, M. Sakamoto, K. Tsutsui and Y. Yazawa, *Bifacial silicon solar cells with 21.3 % front efficiency and 18.8 % rear efficiency*, Prog. Photovolt. Res. Appl. **8**, 385 (2000)

[7] K. J. Weber, A. W. Blakers, P. N. K. Deenapanray, L. A. Sadkowsky, V. Everett and J. Babaei, *The effect of bifacial Sliver® module orientation on energy production*, Proc. 19th European Photovoltaic Solar Energy Conference, 2792 (2004)

[8] J. W. Müller, A. Merkle, R. Hezel, *The Back OECO solar cell: A rear contacted, bifacially sensitive and industrially feasible solar cell with efficiencies of 21.5 %*, Proc. 20th European Photovoltaic Solar Energy Conference, 1020 (2005)
[9] R. Hezel and A. Metz, *A new strategy for the fabrication of cost-effective silicon solar cells*, Renewable Energy, **14**, 83 (1998)
[10] DESSIS, TCAD Manual 6.0.1, Synopsys, Mountain View, CA, 2006.
[11] R. Meyer, P. Engelhart, B. Terheiden , R. Brendel, *A process sequence for silicon solar cells with local boron diffused back surface field*, Proc. 21st European Photovoltaic Solar Energy Conference, 713 (2006)
[12] OptiCAD Corporation, 511 Juniper Drive, Santa Fe NM, www.opticad.com
[13] C. A. Gueymard, 'Parameterized transmittance model for direct beam and circumsolar spectral irradiance', Solar Energy 71(5), 325–346 (2001).
[14] C. A. Gueymard, 'The sun's total and spectral irradiance for solar energy applications and solar radiation models', Solar Energy 76, 423–453 (2004).
[15] ASTM International, 'E490-00a standard solar constant and zero air mass solar spectral irradiance tables', http://www.astm.org (2000).